



UNIVERSITY OF LEEDS

This is a repository copy of *Polymer Molecular Weight Dependence on Lubricating Particle-Particle Interactions*.

White Rose Research Online URL for this paper:
<http://eprints.whiterose.ac.uk/128652/>

Version: Accepted Version

Article:

Yu, K, Hodges, C, Biggs, S et al. (2 more authors) (2018) Polymer Molecular Weight Dependence on Lubricating Particle-Particle Interactions. *Industrial and Engineering Chemistry Research*, 57 (6). pp. 2131-2138. ISSN 0888-5885

<https://doi.org/10.1021/acs.iecr.7b04609>

© 2018 American Chemical Society. This document is the Accepted Manuscript version of a Published Work that appeared in final form in *Industrial and Engineering Chemistry Research*, copyright © American Chemical Society after peer review and technical editing by the publisher. To access the final edited and published work see <https://doi.org/10.1021/acs.iecr.7b04609>

Reuse

Items deposited in White Rose Research Online are protected by copyright, with all rights reserved unless indicated otherwise. They may be downloaded and/or printed for private study, or other acts as permitted by national copyright laws. The publisher or other rights holders may allow further reproduction and re-use of the full text version. This is indicated by the licence information on the White Rose Research Online record for the item.

Takedown

If you consider content in White Rose Research Online to be in breach of UK law, please notify us by emailing eprints@whiterose.ac.uk including the URL of the record and the reason for the withdrawal request.



eprints@whiterose.ac.uk
<https://eprints.whiterose.ac.uk/>

Polymer molecular weight dependence on lubricating particle-particle interactions

Kai Yu¹, Chris Hodges¹, Simon Biggs², Olivier J. Cayre¹, and David Harbottle^{1*}

¹ School of Chemical and Process Engineering, University of Leeds, UK

² Faculty of Engineering, Architecture and Information Technology, The University of Queensland, Australia

ABSTRACT

Using ultra-thin surface coatings of water-soluble polymers to modify interfacial friction is relatively new, but may offer routes to form beneficial coatings whilst using significantly lower polymer concentrations. In the current study, silica surfaces were modified by the physisorption of poly(vinylpyrrolidone) (PVP) from water solution. Four polymer samples with different molecular weights ranging from 8 kDa to 1300 kDa, were examined here. Optical reflectivity measurements showed that the saturated surface excess for each PVP sample was $\sim 1 \text{ mg/m}^2$. The amount of trapped water within the 8 kDa PVP film ($\sim 10 \text{ wt\%}$) was found to be much less than the trapped water (40-55 wt%) in films formed from higher molecular weight PVPs (40 kDa, 360 kDa, and 1300 kDa). In addition, QCM dissipation values for the 8 kDa PVP film was more than four times smaller than those measured for the higher molecular weight PVPs, suggesting that the 8 kDa PVP conforms to a flat film (predominantly train orientation), while the high molecular weight PVPs slowly reorganize resulting in more lossy films (increased Sauerbrey film thickness).

Colloid-probe AFM lateral force measurements showed that 8 kDa PVP films exhibited similar lateral resistance to that seen for uncoated silica surfaces in water, whereas higher molecular weight PVP films showed significantly reduced lateral forces. This lubrication effect, induced by the adsorbed higher molecular weight PVP samples was explored further by measuring the rheology of concentrated particle suspensions. Suspension yield stress data for PVP-coated particles showed a reduction by a factor of 2 in the yield stress when compared to the uncoated particles for suspension concentrations above 60 vol%, i.e. approaching the close-packed limit of spheres.

INTRODUCTION

Friction reduction is important to both traditional industry (e.g. bearing lubrication) and advanced micro- or nano-scale devices such as implants or bio-sensors, from the perspective that reduced friction improves energy utilization and minimizes wear.¹⁻³ Current opinions of friction have been commonly considered in terms of different energy dissipation pathways as the contacting surfaces move past each other, either by thin fluid films or, for surfaces in contact, by molecular species forming boundary layers.⁴ Moreover, lubrication using more environmentally friendly, water-based solvents is increasing in popularity.⁵ Various systems, ranging from micro/nano-electromechanical systems and biomedical devices, to articulating joints or the eye, require surfaces in contact to slide easily past each other in aqueous environments.^{1, 4}

In particular, polymer coatings have been shown to be economic, versatile and convenient approaches to reduce the frictional forces between surfaces in an aqueous system, as they are able to sustain large normal loads while retaining a stable fluid interfacial layer.^{6, 7} The morphology of

the adsorbed or grafted polymer layers and the nature of their interactions with the surfaces, with the solvent, and with each other determine the degree of lubrication.⁸⁻¹⁰ In a good solvent condition, the interactions between two surfaces that are fully coated by polymers (adsorbed or grafted) are usually repulsive due to the osmotic pressure exerted by the confined polymer chains.⁶ Grafted polymer brushes, for example, show negligible mutual interpenetration as they are compressed to $D < 2L_0$ (D is the distance between two surfaces, and L_0 is the mean uncompressed thickness), because of excluded-volume/entropic effects.¹¹ Even under moderate compression, the depletion zone where frictional dissipation occurs remains fluid. The combination of a limited mutual interpenetration of the brushes and a fluid interface results in excellent lubrication (also called entropic lubrication).¹² Recent research emphasized the importance of the interfacial fluid film as well as the morphology of polymer layers on the resultant friction forces.¹³ The interfacial fluid layer may act as a shear plane between polymer brushes (grafted), despite moderate brush collapse, resulting in lower frictional forces. As the solvent quality is further decreased, the brushes undergo significant collapse, and the fluid film at the interface can no longer be maintained. The shear plane then moves to the entangled polymer layers, leading to higher friction coefficients. Similar transitional behaviour has also been shown by polymer films that were formed via physisorption: a low boundary friction coefficient was measured for highly hydrated viscoelastic surface layers, whereas (very) thin adsorbed rigid polymer films had negligible effect on interfacial lubrication.¹⁴ The lubrication effects of polymer coatings are not only confined to reduce the frictional forces between flat surfaces, but also in bulk systems where the rheology of high volume fraction polymer-coated particles can be manipulated by the degree of lubrication. It has been shown that thick and highly hydrated polymer layers strongly repel each other to provide sufficient lubrication for particles to easily slide past one another, resulting in low suspension viscosities.¹⁵

In particular, being a biocompatible, water-soluble, and low-cost polymer, PVP has wide applications in food industries, nanoparticle synthesis, cosmetics, medical and pharmaceutical industries.¹⁶⁻¹⁸ For instance, owing to its good biocompatibility, PVP has been used as a serum albumin substitute,¹⁹ a component of artificial tears and an ingredient of bactericidal iodine.⁵ Recently, PVP has been shown to be a promising lubrication additive for artificial joints by significantly reducing the friction coefficient, as well as improving wear resistance of the joint pairs.^{5, 20} A 2-fold reduction in the coefficient of friction and a 30% reduction in the wear scar diameter relative to water were measured for PVP solutions under a normal load of 2 kN.⁵ PVP also exhibits high degradation resistance, which is beneficial from a tribology perspective, confirming the polymer stability as a lubricant over extended periods of time.

To the best of our knowledge, the lubricating properties of ultra-thin PVP films prepared via physisorption has not previously been considered.²¹ Polymer physisorption is usually simpler than chemical grafting onto surfaces, which can obviously be advantageous when considering routes for efficient and cost effective scale-up. In the current study, surface modification was achieved by adsorbing PVP on silica at ultralow concentrations (≤ 1 ppm). The adsorption behaviour of PVP was studied by optical reflectometry (OR) and Quartz Crystal Microbalance with Dissipation monitoring (QCM-D): allowing us to measure or infer the surface excess, adsorption kinetics, polymer rearrangement on the substrate, and PVP film hydration. The lubricating properties of these adsorbed PVP films at the silica-water interface were measured using an atomic force microscope (AFM). The resultant lubrication effect was subsequently highlighted by measuring the suspension rheology of uncoated and PVP-coated silica particles.

MATERIALS AND METHODS

Materials. PVP (8 kDa, 40 kDa, 360 kDa and 1300 kDa) was purchased from Alfa Aesar (UK). Silicon wafers with a 100 nm thermally deposited oxide layer were purchased from University Wafer (USA). Hollow silica particles (diameter 9 – 13 μm and density $\sim 1.1 \text{ g/mL}$) were purchased from Sigma-Aldrich (UK). Milli-Q water with a resistivity of 18.2 $\text{M}\Omega\cdot\text{cm}$ was used throughout the study.²²

Fixed angle optical reflectometry (OR). PVP adsorption was studied by fixed angle optical reflectometry (OR). The OR has a polarized red He-Ne laser (632.8 nm) that is incident onto a silicon wafer close to the Brewster angle. The intensity of the reflected parallel (R_p) and perpendicular (R_s) components of the laser was monitored by a pair of photodetectors mounted at 90° to each other. R_p/R_s produces a value for the measured signal, S , and changes to this signal, ΔS , are measured during an experiment. Silicon wafers were cut to dimensions of $1 \text{ cm} \times 3 \text{ cm}$ and fresh substrates were used for each experiment. These silicon substrates were UV-Ozone cleaned for 30 min and rinsed with Milli-Q water before positioning the substrate in the flow cell of the OR. Milli-Q water was used as a background liquid to first ensure a stable baseline signal (S_0) before each adsorption experiment, and the change in the measured signal $\Delta S = S - S_0$ was then recorded after PVP solutions were injected.²³ Once a stable surface excess value was obtained, Milli-Q water was re-injected into the OR cell to investigate the rinse-off behaviour of PVP. The adsorbed amount, Γ , can be calculated from, $\Gamma = \frac{\Delta S}{S_0} Q$, where Q is a sensitivity coefficient based on a four-layer optical model.²⁴ After each experiment, the remaining liquid was removed from

the OR cell using a 20 mL syringe, before the OR cell was cleaned by continuously rinsing with 2 L of Milli-Q water.

Quartz crystal microbalance with dissipation monitoring (QCM-D). The adsorption of PVP on silica was also studied using an E4 QCM-D from Q-Sense (Gothenburg, Sweden). The measurement cell is mounted on a Peltier element to provide accurate temperature control (25 ± 0.02 °C). The quartz crystal oscillators (sensors) used for the experiments had a diameter of 14 mm and a fundamental shear oscillation frequency of 5 MHz. The sensors were first cleaned by sonicating in a 2 wt% Decon solution for 30 min followed by 10 min sonication in Milli-Q water, after which the sensors were air dried and left in a UV-Ozone cleaner (Bioforce Nanoscience, USA) for 3 h to eliminate remnant organics.²⁵ All measurements began by running Milli-Q water as a background fluid, before the PVP solution was pumped into the sensor cell after establishing a stable baseline. The changes in frequency (Δf) and dissipation (ΔD) were measured simultaneously at different overtones. In the current study, Δf_3 and ΔD_3 were used to present the frequency and dissipation shifts, since the third overtone provides the best signal-to-noise ratio.

At resonance, an oscillating electric field induces mechanical shear waves in the sensor. Any increase in mass (Δm) on the quartz sensor causes the oscillation frequency of the sensor to decrease, leading to a negative shift in the resonance frequency ($-\Delta f$). According to the Sauerbrey model,²⁶ $\Delta f = -n \frac{1}{C} \Delta m$, where C is the mass sensitivity constant ($C = 17.7 \text{ ng cm}^{-2} \cdot \text{Hz}^{-1}$ at 5 MHz), and n is the overtone number ($n = 1, 3, \dots$). Using the Sauerbrey model, a rigid, non-slip, evenly distributed film is hypothesized. Meanwhile, the QCM-D can also measure the dissipation changes, $\Delta D = 2\Delta\Gamma/f_0$, where $\Delta\Gamma$ is the change in the half-bandwidth of the QCM frequency

spectrum and f_0 is the fundamental resonant frequency of the QCM sensor.²⁷ The measurement of dissipation provides the possibility of estimating the surface excess of viscous films using the Voigt model²⁶ provided by Q-Tools (assuming the density and viscosity of the hydrated PVP film are $1 \times 10^3 \text{ kg/m}^3$ and $1 \times 10^{-3} \text{ Pa}\cdot\text{s}$, respectively). For comparison, both the Sauerbrey and the Voigt models were used to estimate the surface excess of the adsorbed PVP films.

Atomic Force Microscopy (AFM). A BioScope II AFM (Bruker, USA) was used to measure the lateral forces between silica-silica surfaces and PVP-PVP coated silica surfaces using the colloid probe technique. Tipless silicon nitride cantilever (DNP-020, Bruker AFM Probes International Inc., USA) with a spring constant of 0.6 N/m, determined by the thermal resonance method, was used to create colloid probes. Silica particles (Duke Scientific, USA) of 30 μm diameter were attached to the cantilevers using a two-part epoxy glue (Araldite 2012, UK) which was allowed to cure overnight. These colloidal probes were then examined by scanning electron microscopy (Hitachi TM3030, UK) to ensure that the particle was well centred and cleanly attached to the cantilever. Four pieces of silicon wafer were cut and cleaned as aforementioned and were soaked in 1 ppm PVP solutions of different molecular weight (8 kDa, 40 kDa, 360 kDa, and 1300 kDa) for 30 min to ensure the silica surfaces were completely saturated with PVP molecules, after which the silicon wafers were rinsed with Milli-Q water to remove excess PVP. In the same way, four different PVP-coated colloid probes were also prepared. Lateral force measurements were obtained immediately after the PVP surface preparation to ensure that both PVP surfaces remained fully hydrated. These experiments involved depositing two or three drops of Milli-Q water onto the PVP-coated substrate before immersing the colloid probe into the solution. Friction loops were obtained as a function of the normal load (0.44 μN to 2.22 μN) at a

scan length of 1 μm and a scan rate of 1 $\mu\text{m/s}$. All force curves were collected at 0.5 Hz at a minimum of three different surface sites to ensure representative behaviour.

Suspension preparation and bulk rheology. To prepare the uncoated silica particle suspension, 50 g of silica (9 - 13 μm) was added to 50 g of Milli-Q water under gentle agitation, creating a 50 wt% suspension. The suspension concentration was then increased by gradually removing the supernatant by centrifuging the sample at 10,000 rpm. The PVP-coated particle suspensions were prepared by blending 50 g of silica in 50 g of 0.2 wt% solutions of either 8 kDa or 40 kDa PVP (PVP concentration in excess to achieve surface saturation). The PVP-silica suspension was continually mixed for 12 h to ensure uniform PVP coverage on the silica particles before centrifugation and then removing the supernatant. These suspensions were then re-dispersed in Milli-Q water, readjusting the suspension concentration to 50 wt%. The washing process was repeated several times to ensure that any excess PVP was removed.²² Once the 50 wt% suspension containing PVP-coated particles was prepared, the suspension concentration could be increased using the same centrifugation method as for the uncoated particle suspensions.

Flow curves of silica particle and PVP-coated particle suspensions were measured using a stress-controlled Discovery Hybrid Rheometer (DHR-2, TA Instruments, UK) equipped with a cross-hatched plate geometry (40 mm plate). Prior to each measurement the plate geometry was cleaned in acetone and washed with excess Milli-Q water. Sand paper of Grade 40 was fixed to the center of the base plate to prevent suspension slippage, and a solvent trap was used to minimize the evaporation of the suspension liquid. For the flow curve measurements, ~ 2 mL of the suspension was placed on the Peltier plate and the plate geometry lowered to a 1 mm gap setting. With the geometry positioned, a pre-shear protocol of 50 s^{-1} for 60s was executed to ensure that the

suspension structure was not influenced by sample handling and/or history. The suspension rheology was then measured by varying the shear rate between 0.1 and 200 s⁻¹. The measured flow curves were analyzed using the Herschel-Bulkley model to obtain values of yield stress at each suspension concentration. All the measurements were conducted at a constant temperature of 25 °C.

All experiments using the techniques described were repeated at least three times to ensure representative behavior. Average values and errors are reported based on steady-state conditions. Experiments were conducted at 25°C and pH ~ 6.2 (pure Milli-Q water).

RESULTS AND DISCUSSION

PVP surface excess. The adsorption isotherm for 40 kDa PVP at 25°C obtained using the OR is shown in Fig. 1(a). These data indicate two distinct regions for: (i) increasing values of surface excess up to a PVP concentration of 0.1 ppm, and then (ii) a plateau surface excess of ~ 0.9 mg/m² for PVP concentrations \geq 0.1 ppm, correlating well with previously published data.^{22, 28-30} Comparative isotherms for 8 kDa, 40 kDa, 360 kDa and 1300 kDa PVP are presented in Fig. 1(b) and show similar behavior, although the plateau surface excess values are partly dependent on the molecular weight, which is commonly observed for linear polymers.³¹

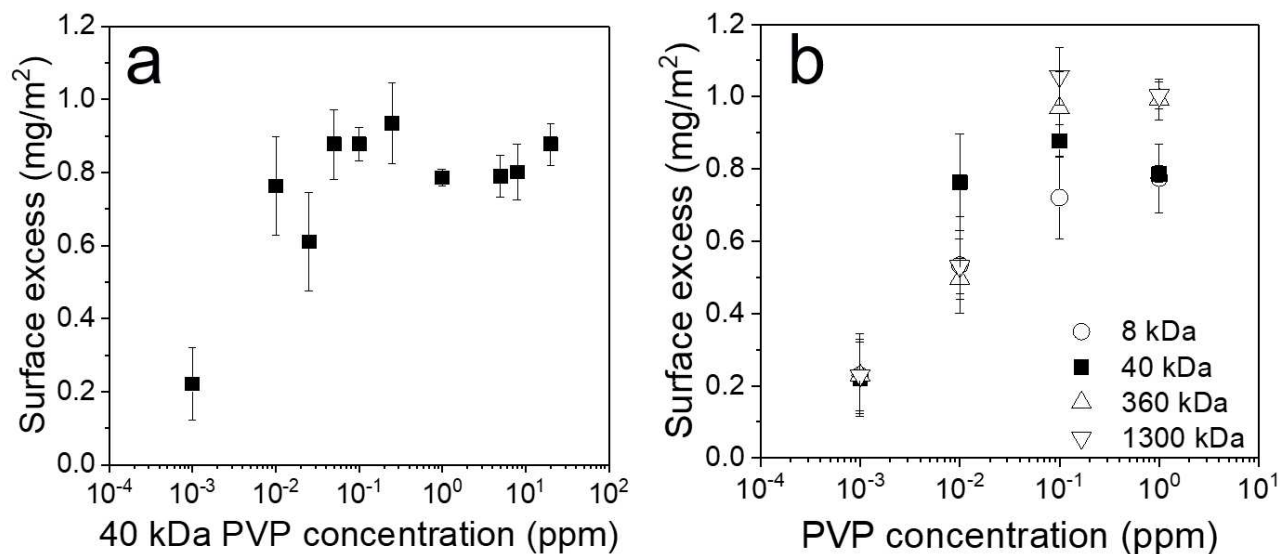


Figure 1. Surface excess isotherms for (a) 40 kDa PVP and (b) comparative isotherms for 8 kDa, 40 kDa, 360 kDa and 1300 kDa PVP measured by OR at 25 °C.

PVP adsorption kinetics. Fig. 2 shows adsorption kinetic data for the 8 kDa PVP sample at a variety of concentrations. Each OR experiment begins by establishing a baseline (approximately 10 min) in Milli-Q water before the PVP solution is injected into the measurement cell. A clear concentration dependence for the PVP adsorption rate exists, with equilibrium surface excess values being achieved after 5 min at 1 ppm PVP but needing more than 1 h at 0.01 ppm PVP. The adsorption rate for 0.001 ppm PVP had the largest uncertainty due to the poor signal-to-noise ratio at this ultra-low concentration, although a repeatable equilibrium surface excess of around 0.2 mg/m² was measured. Once the equilibrium surface excess was obtained, Milli-Q water was re-introduced into the OR cell at the times indicated by the arrows in Fig. 2. Negligible rinse-off of the adsorbed PVP was observed at all concentrations, indicating that the PVP molecules were strongly bound to the silica surface, hence the adsorption of PVP onto silica can be regarded as

being essentially irreversible (over the timescales of interest).³² The initial adsorption rates for different molecular weight PVP and at different polymer concentrations are shown in Fig. S1.

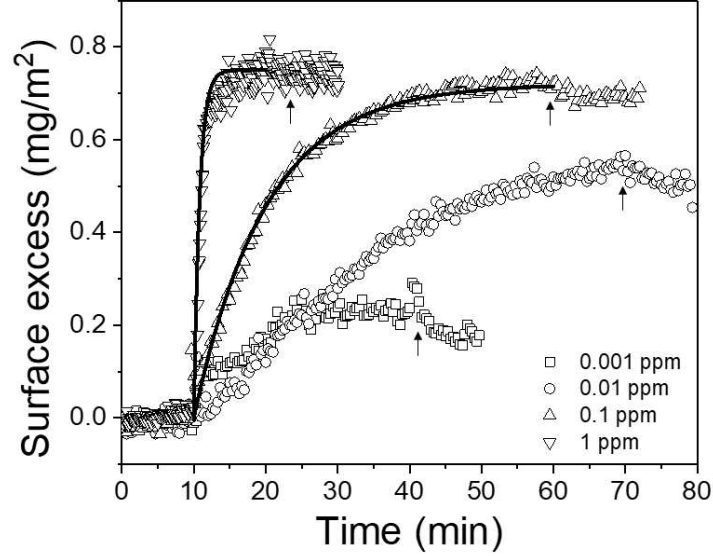


Figure 2. Adsorption kinetics for 8 kDa PVP as a function of the PVP concentration measured by OR. Adsorption kinetics described by Eq. 3 are shown as solid lines. Arrows indicate the injection time of Milli-Q water (rinse-off).

Since PVP adsorption on silica was found to be effectively irreversible, the adsorption kinetics of PVP can be described by relating the changing rate of the surface excess as a function of time t and the initial concentration c of PVP in solution as³¹

$$\frac{d\Gamma}{dt} = k_a c B(\Gamma), \quad (1)$$

where k_a is the adsorption rate coefficient of PVP and $B(\Gamma)$ is the blocking function, which is suggested by the Langmuir model to be³¹

$$B(\Gamma) = \begin{cases} 1 - \Gamma/\Gamma_0, & \Gamma < \Gamma_0 \\ 0, & \Gamma \geq \Gamma_0, \end{cases} \quad (2)$$

where Γ and Γ_0 are the surface excess at time t and at saturation respectively.³¹ The relationship between Γ and the adsorption time can then be calculated by integrating Eq. 1 to give

$$\Gamma = \Gamma_0 - \exp\left(-\frac{k_a ct}{\Gamma_0}\right) \Gamma_0. \quad (3)$$

Comparisons between the experimental data and the kinetic model are shown in Fig. 2 for the 8 kDa PVP. Excellent agreement is obtained for the 0.1 and 1 ppm PVP with an optimal fitting parameter of $k_a = 1.2 \times 10^{-5}$ m/s. However, poor agreement between the experimental data and the kinetic model was observed at lower PVP concentrations, most likely due to an insufficient polymer concentration, i.e. sub-monolayer coverage.³¹ The fitting parameters (k_a) for the 40 kDa, 360 kDa, and 1300 kDa PVP are 8.6×10^{-6} m/s, 5.5×10^{-6} m/s, and 5.0×10^{-6} m/s respectively (Fig. S2), similar in magnitude to reported data for other linear polymers.³¹

PVP film hydration. Complementing the OR data, PVP adsorption was also studied using QCM-D. The main difference between the two techniques is that QCM-D is sensitive to both the adsorbed PVP and any solvent trapped within the adsorbed film (i.e. an apparent film mass), whereas the OR is sensitive only to the adsorbed PVP (i.e. the real polymer film mass). Therefore, by comparing the QCM-D and OR data it is possible to estimate the degree of adsorbed film hydration.³³

The raw QCM-D data was converted to adsorbed surface excess using two different models i) Sauerbrey³⁴ and ii) Voigt³⁵, see Fig. S3. In both models the background fluid is Newtonian with only the thin adsorbed polymer film modelled differently. It can be seen (Fig. S3) that the viscoelastic Voigt model and the elastic Sauerbrey model differ by around 10%, indicating that the adsorbed PVP films mainly behave as an elastic film. Hence the Sauerbrey model is adequate,

and is used for the following analysis. The raw QCM-D data (Δf and ΔD) is shown in the Supporting Information (Fig. S4).

Adsorption of 1 ppm PVP on silica using OR and QCM-D is directly compared in Fig. 3. 1 ppm was chosen since the adsorption isotherms in Fig. 1 confirmed surface saturation at PVP concentrations ≥ 0.1 ppm. Fig. 3 shows that for all QCM-D data, the equilibration time was significantly longer than was observed for the equivalent OR data, most likely due to conformational rearrangement/reorganization of the polymer chains at the solid-liquid interface post adsorption, something for which the OR is insensitive. The QCM-D data also showed little or no rinse-off (Milli-Q water wash identified by the arrows), confirming the findings from the OR experiments (Fig. 2).

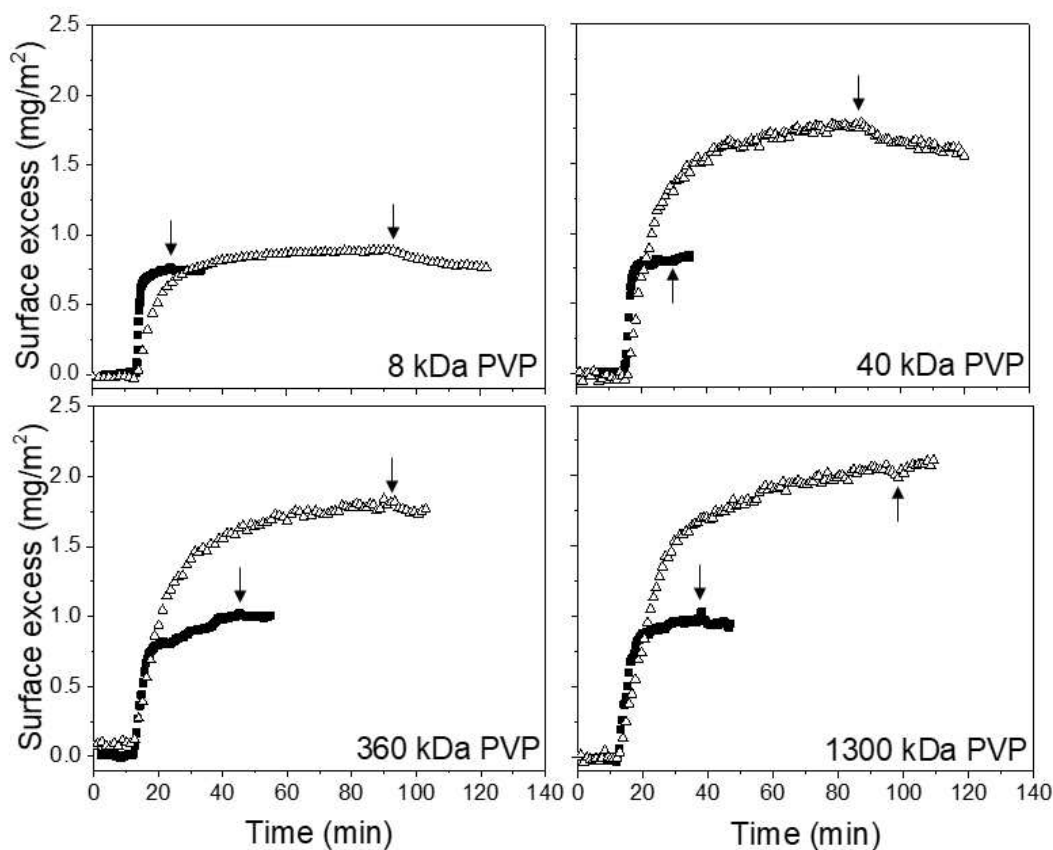


Figure 3. Adsorption kinetics for 1 ppm PVP of different molecular weight measured by OR (closed squares) and QCM-D (open triangles). Arrows indicate the injection time of Milli-Q water (rinse-off).

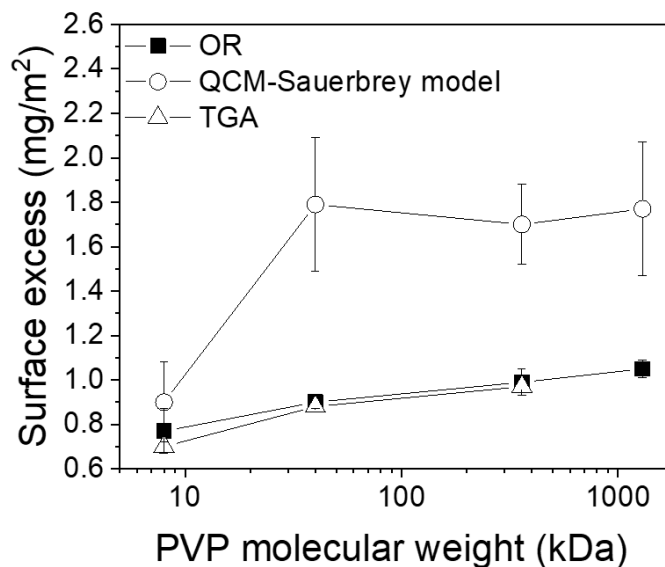


Figure 4. Equilibrium surface excess as a function of the PVP molecular weight measured by OR, QCM-D and TGA.

Thermo-gravimetric analysis (TGA) (Q-500, TA Instruments, USA) was also used to determine adsorbed PVP mass on silica particles. The TGA profiles for silica only, PVP only and PVP-coated silica of varying molecular weight PVP are shown in Fig. S6. Readers are referred to Yu et al.²² for the appropriate analysis to determine the polymer surface excess on silica particles. Equilibrium surface excess values as a function of the PVP molecular weight are compared for the OR, QCM-D and TGA techniques, see Fig. 4. The OR data is in good agreement with the TGA data, confirming that the OR data gives the true polymer film mass. The equilibrium PVP surface excess measured by QCM-D (apparent film mass) is shown to be greater than the surfaces excess determined by OR and TGA, albeit the 8 kDa PVP data is in approximate agreement for all three

techniques. Since the PVP concentration is too low to change the density and viscosity of the bulk liquid,³⁶ the QCM-D data indicates that the 8 kDa PVP forms a film with little water trapped within the relatively flat adsorbed PVP chains (predominantly train orientation), while the higher molecular weight polymers form more hydrated films due to a slightly expanded chain conformation (most likely increased tails and loops orientation).³⁷ Based on the differences in surface excess between the OR (or TGA) and QCM-D data, we can estimate that the amount of water retained in the PVP films for 8 kDa PVP is around 10 wt%, and for the higher molecular weight PVPs (40 kDa, 360 kDa, and 1300 kDa) is approximately 40-55 wt%.

PVP Sauerbrey film thickness and conformation. In addition to the frequency shift (Δf), the dissipation shift (ΔD) can also be measured by QCM-D, see Fig. S4. Since the bulk polymer concentration (1 ppm) used here is too low to change the properties of the background liquid,³⁶ the sensor dissipation will mainly result from the viscous losses caused by the adsorbed PVP film itself, including any trapped water within the PVP film.²⁷

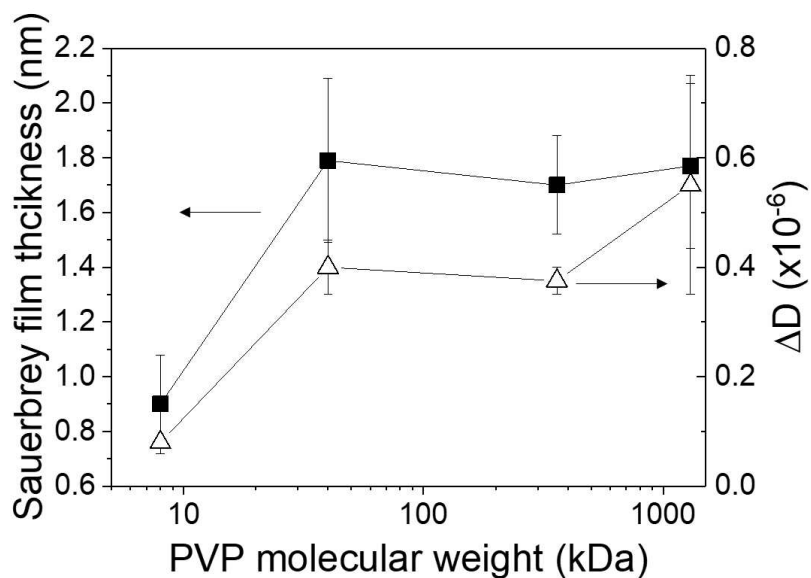


Figure 5. Comparison of the PVP Sauerbrey film thickness and the QCM-D equilibrium dissipation as a function of the PVP molecular weight at 1 ppm.

Fig. 5 shows the relative changes in Sauerbrey film thickness and dissipation as a function of the PVP molecular weight. The average hydrated film thickness determined by QCM-D was ~ 0.9 nm for the 8 kDa PVP film and ~ 1.8 nm for the higher molecular weight PVP films according to the Sauerbrey model. While the Sauerbrey film thickness of the 8 kDa PVP is in good agreement with the average film thickness determined by OR (~ 0.8 nm), when compared for the higher molecular weight PVPs there is significant divergence of the measured film thicknesses (OR data ~ 1 nm for the 40 kDa, 360 kDa and 1300 kDa PVP films). These differences likely result from the degree of PVP film hydration. Considering that the radius of gyration (R_g) of these polymers in solution are ~ 4 nm, ~ 7 nm, ~ 27 nm and ~ 51 nm for 8, 40, 360 and 1300 kDa PVP respectively³⁸, the film thickness data shown in Fig. 4 seem to correspond to conformations where the PVP chains are lying flat or nearly flat on the substrate (PVP chain width previously reported to be ~ 1 nm).³⁹ This likely polymer orientation on the substrate is also justified by the low dissipation values, although

it is worth noting that the dissipation of the 8 kDa PVP film is four times smaller than the higher molecular weight PVPs, signifying increased film stiffness by the lowest molecular weight PVP.

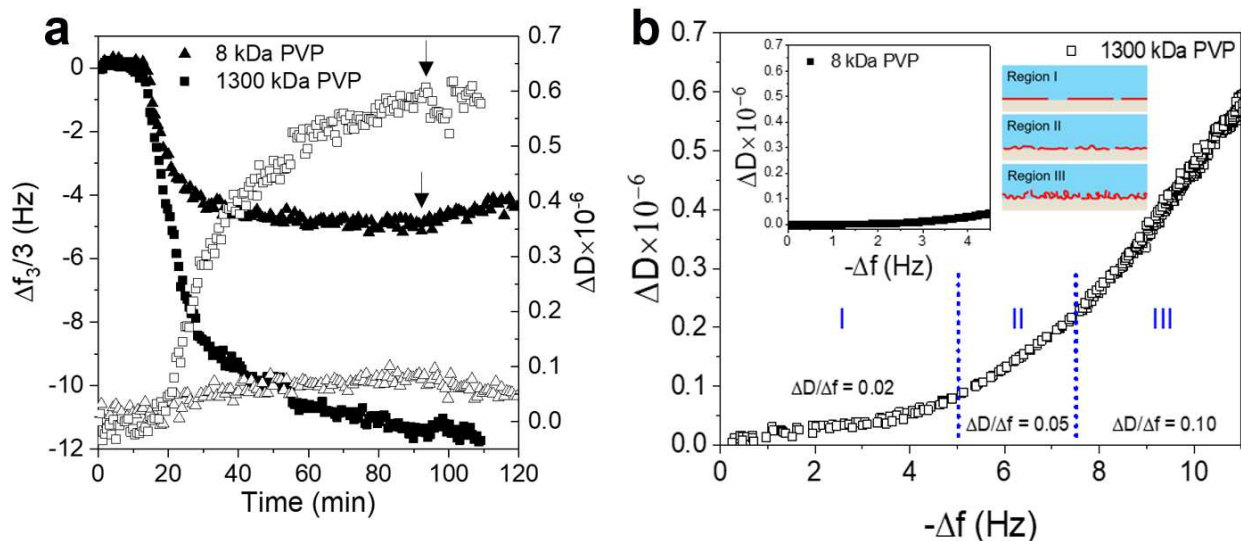


Figure 6. a) Time dependent resonance frequency (closed symbols) and dissipation (open symbols) for 8 kDa and 1300 kDa PVP at 1 ppm. Arrows indicate the injection time of Milli-Q water (rinse-off). b) ΔD as a function of Δf for the 1300 kDa and 8 kDa PVP (shown inset) at 1 ppm. All the $\Delta D/\Delta f$ values shown should be multiplied by a factor of 10^{-6} . Schematic to show the likely polymer orientation to reach the equilibrium state.

Fig. 6b shows ΔD as a function of Δf for the 8 kDa (inset) and 1300 kDa PVP adsorption, highlighting potential conformational changes of the PVP molecules on silica during the adsorption process (rinse-off data not included). Both experiments were allowed to reach equilibrium and the raw data is shown in Fig. 6a. In Fig. 6b the QCM-D response for the 1300 kDa PVP can be divided into three stages, labelled as regions I, II and III, according to the mean slope of each region. Region I shows a very small increase in dissipation (up to 0.08×10^{-6}) with a faster increase in frequency, up to 5 Hz, which is approximately half the equilibrium plateau value of 11

Hz (Fig. 6a), suggesting that during the initial stages of adsorption, the 1300 kDa PVP molecules adsorb flat on the silica surface (predominantly train orientation). In regions II and III the slope ($\Delta D/\Delta f$) increases to 0.05×10^{-6} and 0.1×10^{-6} respectively, representing a larger and larger contribution from the sensor dissipation, with relatively small changes in the frequency. These latter stages (regions II and III) represent the gradual rearrangement/reorganization of the 1300 kDa PVP film resulting in a 40-55 wt% hydration (Fig. 4) of the adsorbed polymer film. The increased contribution from the dissipation is further confirmation of gradual film softening (increased hydration) due to the longer time conformational changes of the adsorbed polymer film. These slower dynamics have previously been reported using AFM, where the authors studying the adsorption of 1 ppm PVP on graphite observed that the polymer first adsorbs in an expanded chain conformation before reconfiguring over several hours to reach an equilibrium state that is slightly more globular and rougher.³⁷ Similar softening behaviour was also observed for the 40 kDa and 360 kDa PVP films, see Fig. S5.

By comparison, the entire adsorption process of the 8 kDa PVP (inset Fig. 6b) reasonably compares to region I of the 1300 kDa PVP data. Very small equilibrium values of Δf and ΔD of 5 Hz and 0.1×10^{-6} respectively were measured for the 8 kDa PVP film. The fact that the equilibrium Δf for the 8 kDa PVP film was about half that of the 1300 kDa film, whereas the ΔD value was more than four times smaller, confirms that negligible softening of the 8 kDa film occurs. From the QCM-D data we would expect the 8 kDa PVP film to be more rigid than the higher molecular weight PVP films.

Particle-substrate lateral force. The lateral forces between silica-silica surfaces, and PVP-coated silica surfaces were measured under different normal loads using the AFM colloid probe technique.⁸ The lateral forces between uncoated silica surfaces (Fig. 7) increased almost linearly with increasing normal load (over the range considered), as expected by Amonton's law.⁴⁰ Interestingly, the measured lateral forces between 8 kDa PVP-PVP surfaces closely matched the uncoated silica data at all loads. By contrast, the 40 kDa PVP-PVP, 360 kDa PVP-PVP, and 1300 kDa PVP-PVP surfaces showed significantly smaller lateral forces, and each of these three longer chain PVP polymers showed a similar response independent of the polymer molecular weight. This suggests that above a critical chain length, PVP can reduce the friction between silica surfaces by approximately a factor of 2.

Qualitatively these results complement the adsorption data, where it was shown (Figs. 4-6) that the 8 kDa PVP forms a comparatively more "rigid" film than the more "lossy" higher molecular weight PVP films. The ability to reconfigure and essentially hydrate to produce an interfacial film of increased softness is favorable for lubrication. Under compression the "soft" interfacial film is able to accommodate the normal load and inhibit hard surface contact, something that is less achievable for the lowest molecular weight PVP, which essentially adsorbs in a flat configuration with little retained water in the polymer film. In summary, the AFM data highlights that a critical PVP molecular weight (~ 40 kDa) exists, around which the friction may be reduced by ~50% compared with uncoated silica surfaces.

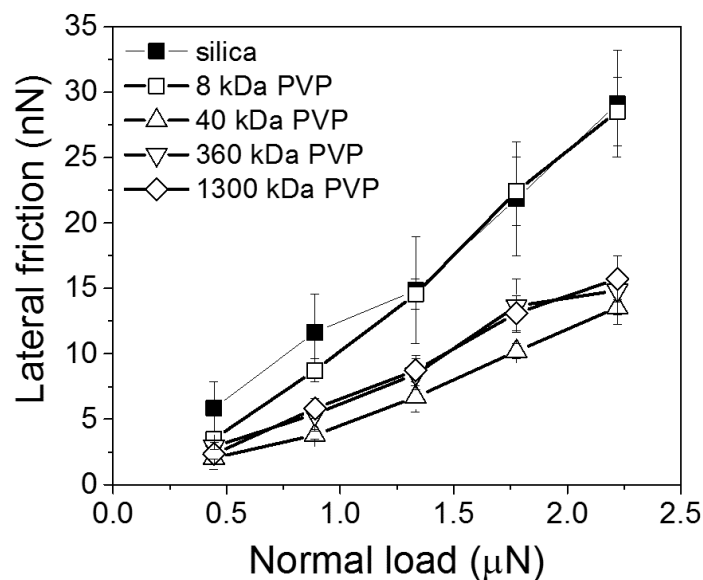


Figure 7. Lateral forces measured between silica-silica, 8 kDa PVP-PVP, 40 kDa PVP-PVP, 360 kDa PVP-PVP, and 1300 kDa PVP-PVP surfaces by a colloid AFM probe.

Yield stress of suspensions. High concentration (50 to 63 vol%) suspensions were prepared using uncoated silica particles in water, as well as 8 kDa PVP and 40 kDa PVP-coated silica particles in water. The rheology flow curves were fitted using the Herschel-Bulkley model to obtain values of yield stress at each suspension concentration (Fig. 8).⁴¹ The Sauerbrey thickness of the PVP film (Fig. 5) was accounted for to shift the ‘apparent’ volume fraction of the composite particle suspension to a slightly higher value (Fig. 8) compared with the uncoated particles. The yield stress of the 40 kDa PVP-coated particle suspension was shown to be significantly reduced above 60 vol% compared with the uncoated silica particle suspension. This result is in broad agreement with the lateral force data (Fig. 7) where it was shown that the 40 kDa PVP films had significantly lower lateral forces than the uncoated silica surfaces. The lubrication effect from a softer polymer film would assist particles to slide past each other more easily when the particles

are highly packed (high contact loading).¹⁵ By contrast, the suspensions prepared using 8 kDa PVP-coated particles behaved similarly to uncoated silica particles, most likely a result of the thin, dehydrated PVP film adsorbed on the particle, as evidenced by OR and QCM-D techniques. This thin and rigid film has much less retained water, resulting in a greater degree of friction between each particle (Fig. 7), and therefore, a larger shear force is needed to induce yielding of the high volume fraction suspension. The diverging response between the uncoated and 40 kDa PVP-coated silica particles resulted from the increased lubrication effect as the apparent particle volume fraction increased. This effect is enhanced at higher particle concentrations as the electrostatic repulsion forces (similar zeta potentials were measured for the uncoated [$\zeta = -41.6 \pm 1.2$ mV] and 1 ppm PVP-coated [$\zeta = -39.1 \pm 1.3$ mV] silica particles) were exceeded by the local contact loads. Fig. 7 showed that significant differences in the lateral friction were measured when the normal load exceeds $0.5 \mu\text{N}$.

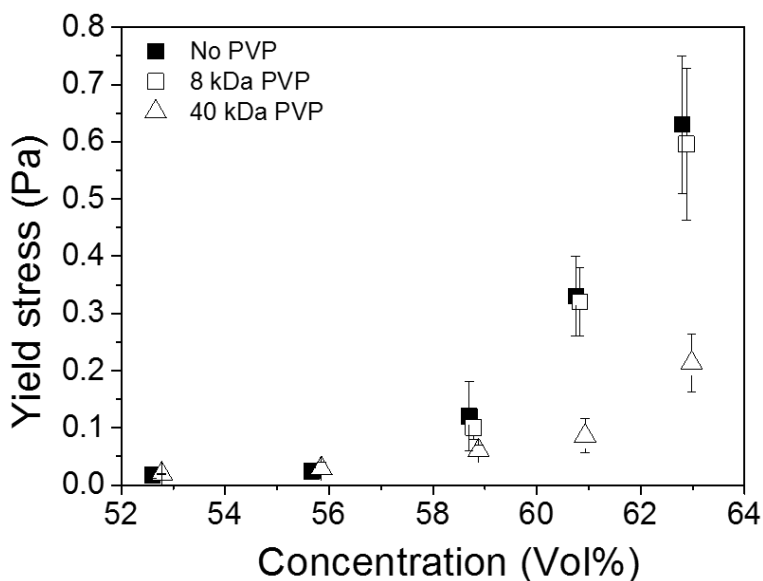


Figure 8: Suspension yield stress as a function of the apparent particle volume fraction for uncoated silica particles (No PVP), 8 kDa and 40 kDa PVP-coated silica particles in water.

CONCLUSIONS

In the current study, silica surfaces were modified by adsorbing poly(vinylpyrrolidone) (PVP) at ultra-low concentrations (≤ 1 ppm). Different PVP molecular weights between 8 kDa and 1300 kDa were used to investigate both the adsorbed mass and the frictional properties of the resultant polymer coating. The surface excess measurements obtained by OR showed a very weak molecular weight dependence, whereas QCM-D data on the same PVP films showed that the amount of retained water in the 8 kDa PVP film was much less (~ 10 wt%) than the retained water in films formed using higher molecular weight PVP (trapped water ~ 40 -55 wt%). Lateral forces measured by AFM between 8 kDa PVP-PVP surfaces very closely matched the uncoated silica lateral forces at all normal loads tested. By contrast, the lateral forces measured between 40 kDa PVP-PVP, 360 kDa PVP-PVP, and 1300 kDa PVP-PVP surfaces were significantly smaller, indicating that above a critical chain length (~ 40 kDa), PVP can significantly reduce the friction between silica surfaces by approximately a factor of 2. The lubrication effect of PVP has been verified by measuring a reduction in the suspension yield stress when the silica particles were coated with 40 kDa PVP. The 8 kDa PVP-coated particles showed negligible variance from the uncoated particles, further validating the lubricating effect of the higher molecular weight PVP at ultra-low polymer concentrations. While the hydration mechanism of the higher molecular weight PVP has not been considered, it is hypothesized that the structural rearrangement of PVP is influenced by the relative bending energy of the higher molecular weight polymers, although such dependence remains to be verified and is the focus of further research.

ACKNOWLEDGMENTS

K.Y. would like to thank the China Scholarship Council, Scholarship No. 201406450027 for supporting this research. The authors would like to acknowledge Professor Anne Neville (University of Leeds) who kindly provided access to the E4 QCM-D.

ASSOCIATED CONTENT

Supporting Information

Initial PVP adsorption rate dependence on the PVP concentration and molecular weight. Semi-log data shown inset (Fig. S1); adsorption kinetics for 40 kDa, 360 kDa and 1300 kDa PVP measured by OR at 1 ppm. Solid lines represent the kinetic model. Arrows indicate the injection time of Milli-Q water (rinse-off) (Fig. S2); PVP molecular weight dependent equilibrium surface excess as determined by Sauerbrey and Voigt models, PVP concentration = 1 ppm (Fig. S3); time dependent frequency and dissipation for 8 kDa, 40 kDa, 360 kDa, and 1300 kDa PVP at 1 ppm (Fig. S4); ΔD as a function of Δf for the 40 kDa and 360 kDa PVP at 1 ppm. All the $\Delta D/\Delta f$ values shown should be multiplied by a factor of 10^{-6} (Fig. S5); TGA profiles for silica nanoparticles, PVP-only, and PVP-coated silica nanoparticles with PVP of increasing molecular weight (Fig. S6). Suspension viscosity (closed symbols) and shear stress (open symbols) as a function of the applied shear rate for a 59 vol% uncoated silica suspension. Dashed line represents the Herschel-Bulkley model used to determine the suspension yield stress (τ), consistency index (k) and flow index (n) (Fig. S7).

AUTHOR INFORMATION

Corresponding Author

David Harbottle; E: d.harbottle@leeds.ac.uk; T: +44 (0)113 343 4154

Notes

The authors declare no competing financial interest.

References

1. Kang, T.; Banquy, X.; Heo, J. H.; Lim, C. N.; Lynd, N. A.; Lundberg, P.; Oh, D. X.; Lee, H. K.; Hong, Y. K.; Hwang, D. S.; Waite, J. H.; Israelachvili, J. N.; Hawker, C. J., Mussel-Inspired Anchoring of Polymer Loops That Provide Superior Surface Lubrication and Antifouling Properties. *Acs Nano* **2016**, 10, (1), 930-937.
2. Li, Y.; Rojas, O. J.; Hinestroza, J. P., Boundary Lubrication of PEO-PPO-PEO Triblock Copolymer Physisorbed on Polypropylene, Polyethylene, and Cellulose Surfaces. *Industrial & Engineering Chemistry Research* **2012**, 51, (7), 2931-2940.
3. Ram, A.; Finkelst.E; Elata, C., Reduction of Friction in Oil Pipelines by Polymer Additives. *Industrial & Engineering Chemistry Process Design and Development* **1967**, 6, (3), 309-&.
4. Jahn, S.; Klein, J., Hydration Lubrication: The Macromolecular Domain. *Macromolecules* **2015**, 48, (15), 5059-5075.
5. Sulek, M. W.; Sas, W.; Wasilewski, T.; Bak-Sowinska, A.; Piotrowska, U., Polymers (Polyvinylpyrrolidones) As Active Additives Modifying the Lubricating Properties of Water. *Industrial & Engineering Chemistry Research* **2012**, 51, (45), 14700-14707.
6. Klein, J., Shear, friction, and lubrication forces between polymer-bearing surfaces. *Annual Review of Materials Science* **1996**, 26, 581-612.
7. Liu, X. M.; Song, J. L.; Wu, D.; Genzer, J.; Theyson, T.; Rojas, O. J., Surface and Friction Behavior of a Silicone Surfactant Adsorbed on Model Textiles Substrates. *Industrial & Engineering Chemistry Research* **2010**, 49, (18), 8550-8557.
8. Dehghani, E. S.; Ramakrishna, S. N.; Spencer, N. D.; Benetti, E. M., Controlled Crosslinking Is a Tool To Precisely Modulate the Nanomechanical and Nanotribological Properties of Polymer Brushes. *Macromolecules* **2017**, 50, (7), 2932-2941.
9. Nomura, A.; Okayasu, K.; Ohno, K.; Fukuda, T.; Tsujii, Y., Lubrication Mechanism of Concentrated Polymer Brushes in Solvents: Effect of Solvent Quality and Thereby Swelling State. *Macromolecules* **2011**, 44, (12), 5013-5019.
10. Dehghani, E. S.; Du, Y. H.; Zhang, T.; Ramakrishna, S. N.; Spencer, N. D.; Jordan, R.; Benetti, E. M., Fabrication and Interfacial Properties of Polymer Brush Gradients by Surface-Initiated Cu(0)-Mediated Controlled Radical Polymerization. *Macromolecules* **2017**, 50, (6), 2436-2446.

11. Wijmans, C. M.; Zhulina, E. B.; Fler, G. J., Effect of Free Polymer on the Structure of a Polymer Brush and Interaction between 2 Polymer Brushes. *Macromolecules* **1994**, *27*, (12), 3238-3248.
12. Witten, T. A.; Leibler, L.; Pincus, P. A., Stress-Relaxation in the Lamellar Copolymer Mesophase. *Macromolecules* **1990**, *23*, (3), 824-829.
13. Nalam, P. C.; Ramakrishna, S. N.; Espinosa-Marzal, R. M.; Spencer, N. D., Exploring Lubrication Regimes at the Nanoscale: Nanotribological Characterization of Silica and Polymer Brushes in Viscous Solvents. *Langmuir* **2013**, *29*, (32), 10149-10158.
14. Stokes, J. R.; Macakova, L.; Chojnicka-Paszun, A.; de Kruif, C. G.; de Jongh, H. H. J., Lubrication, Adsorption, and Rheology of Aqueous Polysaccharide Solutions. *Langmuir* **2011**, *27*, (7), 3474-3484.
15. Starck, P.; Mosse, W. K. J.; Nicholas, N. J.; Spiniello, M.; Tyrrell, J.; Nelson, A.; Qiao, G. G.; Ducker, W. A., Surface chemistry and rheology of polysulfobetaine-coated silica. *Langmuir* **2007**, *23*, (14), 7587-7593.
16. Folmer, B. M.; Kronberg, B., Effect of surfactant-polymer association on the stabilities of foams and thin films: Sodium dodecyl sulfate and poly(vinyl pyrrolidone). *Langmuir* **2000**, *16*, (14), 5987-5992.
17. Kyrychenko, A.; Korsun, O. M.; Gubin, I. I.; Kovalenko, S. M.; Kalugin, O. N., Atomistic Simulations of Coating of Silver Nanoparticles with Poly(vinylpyrrolidone) Oligomers: Effect of Oligomer Chain Length. *Journal of Physical Chemistry C* **2015**, *119*, (14), 7888-7899.
18. Pattanaik, M.; Biswal, S. K.; Bhaumik, S. K., A comparative physicochemical study of hematite with hydroxamic acid and sodium oleate. *Separation Science and Technology* **2000**, *35*, (6), 919-930.
19. Knappe, P.; Bienert, R.; Weidner, S.; Thunemann, A. F., Characterization of poly(N-vinyl-2-pyrrolidone)s with broad size distributions. *Polymer* **2010**, *51*, (8), 1723-1727.
20. Guo, Y.; Hao, Z. X.; Wan, C., Tribological characteristics of polyvinylpyrrolidone (PVP) as a lubrication additive for artificial knee joint. *Tribology International* **2016**, *93*, 214-219.
21. Biggs, S.; Labarre, M.; Hodges, C.; Walker, L. M.; Webber, G. B., Polymerized rodlike micelle adsorption at the solid-liquid interface. *Langmuir* **2007**, *23*, (15), 8094-8102.
22. Yu, K.; Zhang, H.; Hodges, C.; Biggs, S.; Xu, Z.; Cayre, O. J.; Harbottle, D., Foaming Behavior of Polymer-Coated Colloids: The Need for Thick Liquid Films. *Langmuir* **2017**, *33*, (26), 6528-6539.
23. Xu, D.; Hodges, C.; Ding, Y. L.; Biggs, S.; Brooker, A.; York, D., Adsorption Kinetics of Laponite and Ludox Silica Nanoparticles onto a Deposited Poly(diallyldimethylammonium chloride) Layer Measured by a Quartz Crystal Microbalance and Optical Reflectometry. *Langmuir* **2010**, *26*, (23), 18105-18112.
24. de Vos, W. M.; Cattoz, B.; Avery, M. P.; Cosgrove, T.; Prescott, S. W., Adsorption and Surfactant-Mediated Desorption of Poly(vinylpyrrolidone) on Plasma- and Piranha-Cleaned Silica Surfaces. *Langmuir* **2014**, *30*, (28), 8425-8431.
25. Crespo-Quesada, M.; Andanson, J. M.; Yarulin, A.; Lim, B.; Xia, Y. N.; Kiwi-Minsker, L., UV-Ozone Cleaning of Supported Poly(vinylpyrrolidone)-Stabilized Palladium Nanocubes: Effect of Stabilizer Removal on Morphology and Catalytic Behavior. *Langmuir* **2011**, *27*, (12), 7909-7916.

26. Bakhtiari, M. T.; Harbottle, D.; Curran, M.; Ng, S.; Spence, J.; Siy, R.; Liu, Q. X.; Masliyah, J.; Xu, Z. H., Role of Caustic Addition in Bitumen-Clay Interactions. *Energy & Fuels* **2015**, *29*, (1), 58-69.
27. Rodahl, M.; Hook, F.; Fredriksson, C.; Keller, C. A.; Krozer, A.; Brzezinski, P.; Voinova, M.; Kasemo, B., Simultaneous frequency and dissipation factor QCM measurements of biomolecular adsorption and cell adhesion. *Faraday Discussions* **1997**, *107*, 229-246.
28. Pattanaik, M.; Bhaumik, S. K., Adsorption behaviour of polyvinyl pyrrolidone on oxide surfaces. *Materials Letters* **2000**, *44*, (6), 352-360.
29. Goodwin, D. J.; Sepassi, S.; King, S. M.; Holland, S. J.; Martini, L. G.; Lawrence, M. J., Characterization of Polymer Adsorption onto Drug Nanoparticles Using Depletion Measurements and Small-Angle Neutron Scattering. *Molecular Pharmaceutics* **2013**, *10*, (11), 4146-4158.
30. Robinson, S.; Williams, P. A., Inhibition of protein adsorption onto silica by polyvinylpyrrolidone. *Langmuir* **2002**, *18*, (23), 8743-8748.
31. Szilagyi, I.; Trefalt, G.; Tiraferri, A.; Maroni, P.; Borkovec, M., Polyelectrolyte adsorption, interparticle forces, and colloidal aggregation. *Soft Matter* **2014**, *10*, (15), 2479-2502.
32. Stuart, M. A. C.; Fleer, G. J.; Scheutjens, J. M. H. M., Displacement of Polymers .2. Experiment - Determination of Segmental Adsorption Energy of Poly(Vinylpyrrolidone) on Silica. *Journal of Colloid and Interface Science* **1984**, *97*, (2), 526-535.
33. Hodges, C. S.; Biggs, S.; Walker, L., Complex Adsorption Behavior of Rodlike Polyelectrolyte-Surfactant Aggregates. *Langmuir* **2009**, *25*, (8), 4484-4489.
34. Sauerbrey, G., Verwendung Von Schwingquarzen Zur Wagung Dunner Schichten Und Zur Mikrowagung. *Zeitschrift Fur Physik* **1959**, *155*, (2), 206-222.
35. Voinova, M. V.; Rodahl, M.; Jonson, M.; Kasemo, B., Viscoelastic acoustic response of layered polymer films at fluid-solid interfaces: Continuum mechanics approach. *Physica Scripta* **1999**, *59*, (5), 391-396.
36. Kanazawa, K. K.; Gordon, J. G., The Oscillation Frequency of a Quartz Resonator in Contact with a Liquid. *Analytica Chimica Acta* **1985**, *175*, (Sep), 99-105.
37. Fleming, B. D.; Wanless, E. J.; Biggs, S., Nonequilibrium mesoscale surface structures: The adsorption of polymer-surfactant mixtures at the solid/liquid interface. *Langmuir* **1999**, *15*, (25), 8719-8725.
38. Qiu, H.; Bousmina, M., New technique allowing the quantification of diffusion at polymer polymer interfaces using rheological analysis: Theoretical and experimental results. *Journal of Rheology* **1999**, *43*, (3), 551-568.
39. Spruijt, E.; Biesheuvel, P. M.; de Vos, W. M., Adsorption of charged and neutral polymer chains on silica surfaces: The role of electrostatics, volume exclusion, and hydrogen bonding. *Physical Review E* **2015**, *91*, (1).
40. Gao, J. P.; Luedtke, W. D.; Gourdon, D.; Ruths, M.; Israelachvili, J. N.; Landman, U., Frictional forces and Amontons' law: From the molecular to the macroscopic scale. *Journal of Physical Chemistry B* **2004**, *108*, (11), 3410-3425.
41. Dzuy, N. Q.; Boger, D. V., Yield Stress Measurement for Concentrated Suspensions. *Journal of Rheology* **1983**, *27*, (4), 321-349.

Graphical Abstract:

